

# The miR-195 Axis Regulates Chemoresistance through TUBB and Lung Cancer Progression through BIRC5

Xiaojie Yu,<sup>1,2,6</sup> Yiqiang Zhang,<sup>1</sup> Binggen Wu,<sup>1,3</sup> Jonathan M. Kurie,<sup>4</sup> and Alexander Pertselmidis<sup>1,2,5</sup>

<sup>1</sup>Greehey Children's Cancer Research Institute, The University of Texas Health Science Center at San Antonio, San Antonio, TX 78229 USA; <sup>2</sup>Department of Cell Systems and Anatomy, The University of Texas Health Science Center at San Antonio, San Antonio, TX 78229 USA; <sup>3</sup>Xiangya School of Medicine, Central South University, Changsha, Hunan 410000, China; <sup>4</sup>Department of Thoracic/Head and Neck Medical Oncology, The University of Texas MD Anderson Cancer Center, Houston, TX 77030 USA; <sup>5</sup>Department of Pediatrics, The University of Texas Health Science Center at San Antonio, San Antonio, TX 78229 USA

**Chemoresistance and metastasis are the major reasons for non-small cell lung cancer (NSCLC) treatment failure and patient deaths. We and others have shown that miR-195 regulates the sensitivity of NSCLC to microtubule-targeting agents (MTAs) *in vitro* and *in vivo* and that miR-195 represses the migration and invasion of NSCLC cells *in vitro*. However, the relationship between miR-195 and microtubule structure and function and whether miR-195 represses NSCLC metastasis *in vivo* remain unknown. We assessed the correlation between tumor levels of *TUBB* and patient survival, the effect of *TUBB* on drug response, and the effect of miR-195 on migration, invasion, and metastasis *in vitro* and *in vivo*. We found that miR-195 directly targets *TUBB*; knockdown of *TUBB* sensitizes cells to MTAs, while overexpression confers resistance; high expression of *TUBB* is correlated with worse survival of lung adenocarcinoma; *TUBB* is also regulated by *CHEK1*, which has been shown to regulate chemoresistance; and miR-195 targets *BIRC5* to repress migration and invasion *in vitro* and metastasis *in vivo*. Our findings highlight the relevance of the miR-195/*TUBB* axis in regulating the response of NSCLC to MTAs and the importance of the miR-195/*BIRC5* axis in regulating NSCLC metastasis.**

## INTRODUCTION

Lung cancer is the leading cause of cancer deaths worldwide.<sup>1</sup> Around 85% of lung cancer is non-small cell lung cancer (NSCLC), which is histologically classified into lung adenocarcinoma (LUAD), lung squamous cell carcinoma (LUSC), and large cell lung carcinoma. For decades, microtubule-targeting agents (MTAs) have been used in the treatment of NSCLC. Although MTAs have achieved promising results in certain patients, the response rate in NSCLC is very low (~10%–40%), which poses a significant barrier to improving long-term outcomes of NSCLC patients.<sup>2–5</sup> Even in responsive NSCLC patients, resistance usually develops over time, resulting in disease recurrence and metastasis, the latter of which is responsible for 90% of lung cancer deaths.<sup>6</sup> Therefore, it is critical to understand the mechanisms underlying drug resistance and metastasis and the relationships between them.

Multiple mechanisms have been implicated in drug resistance. One common mechanism is selective efflux mediated by membrane-bound ATP-dependent pumps, which pump substrates—toxic metabolites and xenobiotics—into the blood, reducing effective drug concentrations in tumor cells and conferring resistance to a large number of structurally unrelated cytotoxic drugs, including the MTAs.<sup>7–10</sup> Other mechanisms include tubulin mutations, altered microtubule binding dynamics, and impaired centrosome clustering.<sup>11</sup> Changes in tubulin expression have also been shown to contribute to resistance to MTAs.<sup>9,10,12–16</sup> Specifically, overexpression of class III beta-tubulin (*TUBB3*) has been implicated in resistance to paclitaxel in several cancer types, including pancreatic ductal adenocarcinoma, breast cancer, and lung cancer.<sup>15,17–19</sup> In addition, there has been some debate about the role of tubulin beta class I (*TUBB*) in paclitaxel resistance in NSCLC. *TUBB* mutations were first reported to correlate with paclitaxel resistance in NSCLC patients.<sup>20</sup> It was later argued, however, that *TUBB* mutations are not common in NSCLC and that the reported *TUBB* mutations likely occur in *TUBB* pseudogenes.<sup>21–23</sup> No correlation of *TUBB* expression with paclitaxel resistance was found.<sup>17</sup> To date, whether or not *TUBB* plays a role in chemoresistance has not been experimentally determined.

Metastasis is the main cause of cancer deaths and is largely driven by invasion of tumor cells into surrounding tissues and migration of tumor cells to distant sites. Survivin, encoded by the *BIRC5* gene, has been shown to regulate the migration and invasion of various cancer cells, including melanoma, colorectal cancer, oral squamous cell carcinoma, cervical cancer, and breast cancer.<sup>24–29</sup> *BIRC5* is overexpressed in various tumors, with high expression correlating with worse survival.<sup>30,31</sup> Repression of survivin has been proposed as a potential cancer therapy.<sup>32</sup>

Received 23 April 2019; accepted 24 July 2019;  
<https://doi.org/10.1016/j.omto.2019.07.004>.

<sup>6</sup>Present address: Department of Genetics, The University of Texas MD Anderson Cancer Center, Houston, TX 77030 USA.

**Correspondence:** Alexander Pertselmidis, Greehey Children's Cancer Research Institute, The University of Texas Health Science Center at San Antonio, San Antonio, TX 78229 USA.

**E-mail:** [pertselmidis@uthscsa.edu](mailto:pertselmidis@uthscsa.edu)



**Table 1. Expression of Tubulin Isoforms in miR-195-Transfected Cells Relative to Control Cells**

Gene	H358	H1993
TUBB*	0.58	0.64
TUBA1A*	0.64	0.64
TUBB4B*	0.66	0.72
TUBA3D*	0.74	0.79
TUBB4Q	0.81	0.69
TUBG2	0.82	1.08
TUBG1	0.83	0.86
TUBD1	0.84	0.94
TUBA3E	0.85	0.92
TUBA1B	0.86	1.04
TUBA1C	0.87	0.91
TUBA4	0.92	0.85
TUBB1	0.92	1.09
TUBB3	0.95	1.05
TUBB8	0.97	0.96
TUBA8	0.99	0.97
TUBB6	1.00	0.99
TUBB4	1.00	1.08
TUBA3C	1.03	0.97
TUBE1	1.08	1.03
TUBB2B	1.12	0.90
TUBA4A	1.20	0.82
TUBB2A	1.33	1.04

\*These isoforms were down-regulated by miR-195 by at least 20% in both cell lines.

We have recently shown that survivin regulates both apoptosis and senescence in NSCLC cells.<sup>33</sup> However, the role of survivin in regulating the migration and invasion of NSCLC cells has not been fully studied.

microRNAs (miRNAs) are a family of small non-coding RNAs that post-transcriptionally repress gene expression.<sup>34</sup> Among them, miR-195 has been shown to regulate various aspects of cancer, including chemoresistance and metastasis. Specifically, miR-195 increases chemosensitivity of colon cancer<sup>35</sup> and cervical cancer,<sup>36</sup> but correlates with acquired chemoresistance in glioblastoma.<sup>37</sup> We have recently shown that miR-195 targets *CHEK1* to sensitize NSCLC to MTAs.<sup>38</sup> miR-195 has also been implicated as a regulator of cancer metastasis through a few reports showing its regulation of migration and invasion *in vitro*. For example, miR-195 represses cancer cell migration and invasion in esophageal squamous cell carcinoma,<sup>39</sup> breast cancer,<sup>40</sup> NSCLC,<sup>41</sup> osteosarcoma,<sup>42</sup> and hepatocellular carcinoma.<sup>43</sup> In contrast, miR-195 promotes the migration and invasion of melanoma.<sup>44</sup> The actual effects of miR-195 on metastasis *in vivo* have not been established.

Our investigation of the function of miR-195 in NSCLC revealed that *TUBB* is a direct target of miR-195, regulating the response of NSCLC

cells to MTAs and that expression of *TUBB* correlates with the prognosis of NSCLC patients. We also found that miR-195 and *TUBB* had no effect on microtubule structure. Interestingly, we show that *TUBB* expression can be regulated by another target of miR-195, *CHEK1*, which had previously been shown to regulate chemoresistance in NSCLC.<sup>38</sup> Finally, we report that miR-195 represses the metastasis of NSCLC *in vivo* and that its target, *BIRC5*, regulates the migration and invasion of NSCLC cells. Our results not only advance our understanding of the mechanisms of drug resistance and metastasis in NSCLC, but also shed light on strategies for addressing both problems by exploiting a single vulnerability in cancer cells.

## RESULTS

### TUBB Expression Correlates with Prognosis in Lung Adenocarcinoma Patients

We recently demonstrated that miR-195 synergizes with MTAs to repress the growth of NSCLC cells.<sup>38</sup> We subsequently asked whether miR-195 had an effect on microtubules. We re-visited the gene expression profiling of two NSCLC cell lines, H1993 and H358, transfected with miR-195 as we previously reported.<sup>33</sup> We focused on the expression of tubulin isoforms and found that none were down-regulated by at least 2-fold (or 50%) by miR-195 (Table 1). However, four isoforms (*TUBB*, *TUBA1A*, *TUBB4B*, and *TUBA3D*) were down-regulated by miR-195 by at least 20% in both cell lines, encouraging us to further investigate whether these genes are direct targets of miR-195 or participate in the regulation of cellular response to MTAs. We found that high expression of *TUBB*, *TUBA3D*, or *TUBB4B* is correlated with worse overall survival and worse chemotherapy response in lung adenocarcinoma patients (Figures 1A and 1B; Figure S1), as assessed by Kaplan-Meier survival analysis and log-rank test.<sup>45</sup> However, the expression of these genes is not significantly correlated with overall survival or chemotherapy response in lung squamous cell carcinoma patients (Figures 1C and 1D; Figure S2). Among these three genes, we identified a binding site for miR-195 only in the 3' UTR of *TUBB* (Figure 2G). In similar analysis of data from The Cancer Genome Atlas (TCGA), we found that high expression of *TUBB* is correlated with worse overall survival and recurrence-free survival of lung adenocarcinoma, but not squamous cell carcinoma (Figures 1E–1H).

### TUBB Is Targeted by miR-195 and Regulates the Response of Lung Adenocarcinoma Cells to MTAs

*TUBB* is expressed at higher levels in tumor tissues compared to adjacent normal tissues in both lung adenocarcinoma and squamous cell carcinoma patients (Figures 2A and 2B), as shown by analysis of gene expression in TCGA datasets. Specifically, *TUBB* is upregulated in tumor tissues in 51 of 57 lung adenocarcinoma patients and in 49 of 51 lung squamous cell carcinoma patients. Expression of *TUBB* is negatively correlated with miR-195 in lung adenocarcinoma, but not squamous cell carcinoma (Figures 2C and 2D). We demonstrated that this relationship is causal—miR-195 inhibits both the mRNA and protein levels of *TUBB* (Figures 2E and 2F)—and confirmed the direct and specific binding of miR-195 to the 3' UTR of *TUBB* by luciferase assay (Figure 2G). To functionally validate that *TUBB*

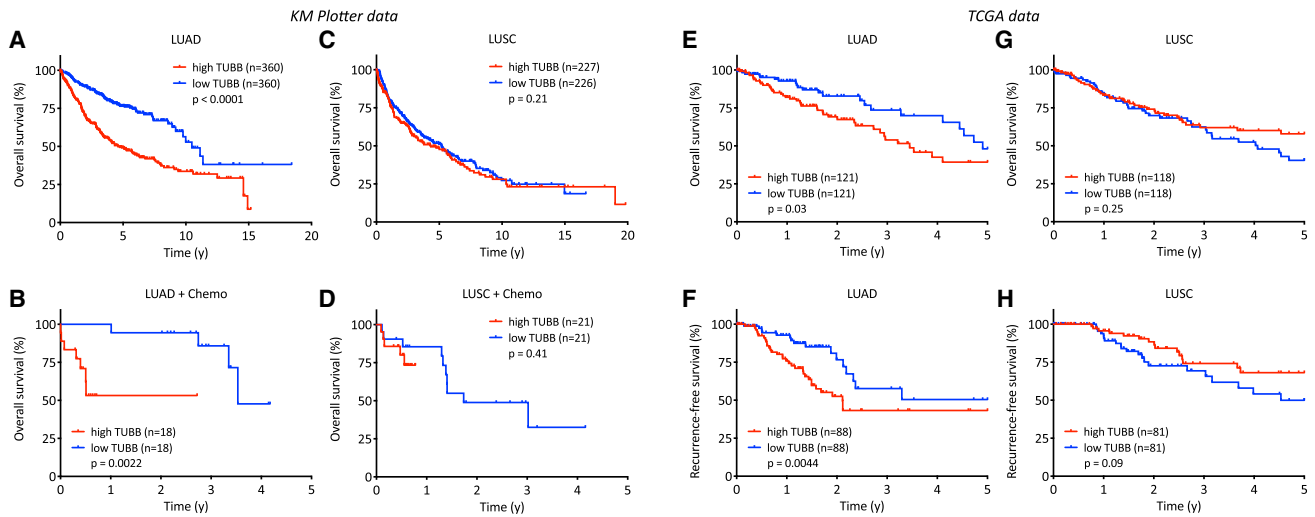


**Figure 1. TUBB Expression Is Correlated with Prognosis of Lung Adenocarcinoma Patients**

(A) 5-year overall survival curves of lung adenocarcinoma patients based on *TUBB* expression. (B) 5-year overall survival curves of lung adenocarcinoma patients treated with chemotherapy based on *TUBB* expression. (C) 5-year overall survival curves of lung squamous cell carcinoma patients based on *TUBB* expression. (D) 5-year overall survival curves of lung squamous cell carcinoma patients treated with chemotherapy based on *TUBB* expression. (A)–(D) were generated from KM Plotter, excluding patients from the TCGA datasets. (E) 5-year overall survival curves of lung adenocarcinoma patients based on *TUBB* expression. (F) 5-year recurrence-free survival curves of lung adenocarcinoma patients based on *TUBB* expression. (G) 5-year overall survival curves of lung squamous cell carcinoma patients based on *TUBB* expression. (H) 5-year recurrence-free survival curves of lung squamous cell carcinoma patients based on *TUBB* expression. (E)–(H) were generated from The Cancer Genome Atlas (TCGA).

regulates the response of lung adenocarcinoma cells to MTAs, we knocked down *TUBB* with a validated siRNA pool designed against *TUBB* (siTUBB)<sup>19</sup> (Figure 3A). We found that knockdown of *TUBB* sensitizes H1299 cells to eribulin, but not paclitaxel, and sensitizes H1993 and A549 cells to both paclitaxel and eribulin (Figures 3B and 3C). Importantly, we demonstrated that overexpression of *TUBB* slightly, but significantly, contributes to the resistance of lung adenocarcinoma cells to paclitaxel and eribulin (Figure 4). Collectively, these results support that *TUBB* is a direct target of miR-195 and regulates the response of lung adenocarcinoma cells to MTAs.

Since we previously demonstrated that miR-195 targets the cell-cycle checkpoint kinase *CHEK1* to sensitize NSCLC cells to MTAs,<sup>38</sup> we next asked whether *CHEK1* could regulate the expression of *TUBB*. Intriguingly, the expression of *TUBB* is significantly correlated with *CHEK1* expression in both lung adenocarcinoma and squamous cell carcinoma patients (Figure 5A). We confirmed that *TUBB* is regulated by *CHEK1*: knockdown of *CHEK1* represses *TUBB* protein levels in H1299 cells, while overexpression of *CHEK1* increases *TUBB* protein levels (Figure 5B).

#### miR-195 Does Not Influence Microtubule Structure

To assess whether miR-195 regulation of *TUBB* affects microtubule structures, we visualized microtubule structures through immunofluorescence staining. We were unable to identify dramatic changes to microtubule structures resulting from either increased levels of miR-195 or decreased levels of *TUBB* (Figure 6; Figure S3). We did

find that paclitaxel and eribulin cause profound microtubule disruption, as expected. Intriguingly, we also found that paclitaxel and eribulin induce multinucleation in cancer cells. We were unable, however, to demonstrate whether miR-195 or siTUBB enhance the effects of paclitaxel and eribulin on microtubule disruption.

#### miR-195 Represses the Metastasis of Lung Adenocarcinoma

Hallmarks of cancer, migration, and invasion greatly promote tumor progression. miR-195 has been demonstrated to repress the growth, migration, and invasion of lung cancer cells.<sup>41,46</sup> However, the observed repression of migration and invasion could not be distinguished from inhibitory effects on cell growth. To control for the cytotoxicity of miR-195, we assessed cell viability while performing transwell migration and Matrigel invasion assays. The number of cells migrating or invading to the other side of membrane was normalized to cell viability, yielding a “relative cell count” for migration and invasion. The results confirmed that miR-195 inhibits the migration and invasion of lung adenocarcinoma cells independent of its effect on cell viability and that miR-195 inhibitors promote migration and invasion of cancer cells, albeit slightly (Figures 7A–7D; Figure S4). In addition, we exploited a chemotaxis assay designed for real-time visualization and automated analysis of cell migration and invasion to show that miR-195 inhibits the migration and invasion of cancer cells (Figures 8A and 8B).

We generated cells stably overexpressing miR-195 (H1299/luc-miR-195 #116 and #126) and demonstrated that constitutive overexpression of miR-195 inhibits cancer cell migration and

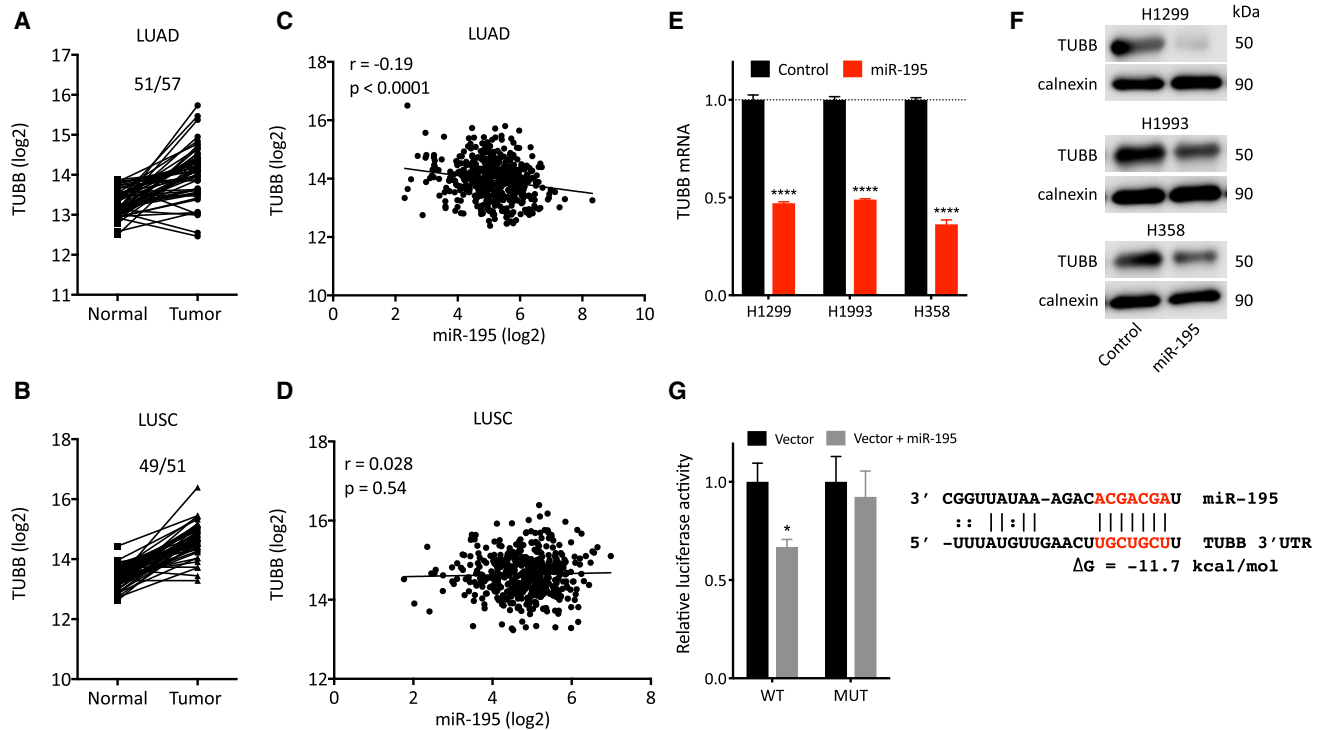


**Figure 2. TUBB Is a Direct Target of miR-195**

(A) Expression of *TUBB* in tumor tissues compared to adjacent normal tissues in lung adenocarcinoma (LUAD). Paired t test,  $p < 0.0001$ . (B) Expression of *TUBB* in tumor tissues compared to adjacent normal tissues in lung squamous cell carcinoma (LUSC). Paired t test,  $p < 0.0001$ . (C) Correlation of *TUBB* with miR-195 in tumor tissues of lung adenocarcinoma ( $n = 508$ ) patients. (D) Correlation of *TUBB* with miR-195 in tumor tissues of lung squamous cell carcinoma ( $n = 476$ ) patients. (E) mRNA levels of *TUBB* in H1299, H1993, and H358 cells transfected with miR-195 mimic. (F) *TUBB* protein levels after transfected with miR-195 mimic for 3–4 days. (G) Predicted binding site between miR-195 and the 3' UTR of *TUBB*. Luciferase reporter assay for direct and specific interaction of miR-195 with the predicted target site in the *TUBB* 3' UTR. Deletion of the target site in the *TUBB* 3' UTR abolishes the inhibition of luciferase activity by miR-195. WT, wild-type; MUT, deleted miR-195 binding site in the *TUBB* 3' UTR. Results are shown as mean  $\pm$  SD. \* $p < 0.05$ ; \*\*\*\* $p < 0.0001$ . Experiments were repeated at least twice.

invasion *in vitro* (Figures S5A–S5E). To assess the effect of miR-195 on experimental metastasis *in vivo*, we injected control cells (H1299/luc-EV) and miR-195 overexpressing cells (H1299/luc-miR-195 #116) intravenously into nude mice. Because these cells express luciferase, we were able to use bioluminescence to visualize cell localization. After 10 weeks, we found lung metastases in 1 of 7 mice in the control group and no lung metastases in the miR-195 overexpressing group (Figures S5F and S5G). It is not clear why metastasis occurred in only one mouse in the control group. We believe this is due to experimental variance with H1299 cells, supported by one report showing that H1299 cells inoculated intravenously did not show lung or other organ metastasis for up to 4 months<sup>47</sup> and another report demonstrating lung metastasis with H1299 cells in only 6 weeks.<sup>48</sup>

Leveraging an experimental model of lung metastasis, mouse lung adenocarcinoma cell line 344SQ, which has been demonstrated to form lung metastases when inoculated subcutaneously into syngeneic mice,<sup>49</sup> we subcutaneously injected 344SQ/control cells and 344SQ cells overexpressing miR-195 (344SQ/miR-195) into syngeneic mice (4 mice in the control group and 5 mice in the miR-195 group)

(Figure S6A). Due to the small number of mice and large variance in tumor size, tumor weight and size in the miR-195 group were not significantly smaller than those in the control group (Figures S6B–S6E). The body weights of the mice were not significantly different between two groups either (Figure S6F). However, we observed lung metastases in 4 of 4 mice in the control group, and in only 1 of 5 mice in the miR-195 group (Figure 7E). Quantification of lung metastasis demonstrated that the number of metastases is significantly smaller in the miR-195 group than in the control group, implying that miR-195 represses lung metastasis *in vivo* (Figures 7F–7H).

#### Survivin Mediates the Role of miR-195 to Regulate the Migration and Invasion of Lung Adenocarcinoma Cells

*BIRC5* has been shown to regulate apoptosis, senescence, migration, and invasion of cancer cells.<sup>25,50,51</sup> We recently demonstrated that miR-195 targets *BIRC5* to induce apoptosis and senescence in NSCLC cells.<sup>33</sup> We were curious whether *BIRC5* also mediates the function of miR-195 to regulate cell migration and invasion. We found that overexpression of *BIRC5* indeed reverses the effects of miR-195 and that knockdown of *BIRC5* inhibits the migration and invasion of cancer

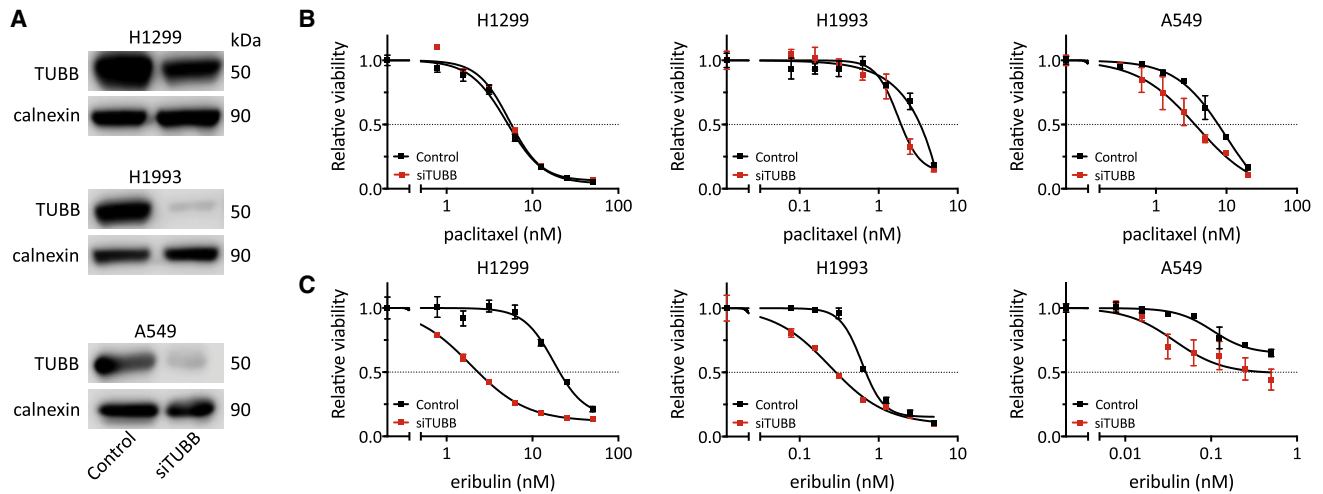


**Figure 3. Knockdown of TUBB Sensitizes NSCLC Cells to MTAs**

(A) Protein levels of TUBB assessed by western blot. (B) Response of cancer cells to paclitaxel with or without TUBB siRNA (siTUBB) treatment. (C) Response of cancer cells to eribulin with or without siTUBB treatment. Results are shown as mean  $\pm$  SD. Experiments were repeated at least twice.

cells, confirming that miR-195 targets *BIRC5* to regulate the migration and invasion of lung cancer cells (Figures 8A–8D). However, we did not find a correlation between miR-195/*BIRC5* expression and tumor stage in TCGA data (Figure S7). We also found that miR-195 has no influence on vimentin and E-cadherin protein levels, indicating that miR-195 probably does not regulate the epithelial-mesenchymal transition of NSCLC cells (Figure S8). Collectively, our data indicate that miR-195/*BIRC5* dysregulation is not a driver of lung metastasis, but a contributing factor.

## DISCUSSION

The capacity to simultaneously target multiple oncogenic pathways potentially enables a tumor suppressor miRNA to therapeutically address cancer heterogeneity. However, concerns have been raised over potential off-target effects, given that any gene possessing the target sequence of a miRNA in its 3' UTR can theoretically be repressed by that miRNA. A complete understanding of the functions and targets of a miRNA in the context of cancer is therefore required for proper evaluation of its clinical potential. miR-195 has been shown to target various cancer-related genes to regulate lung cancer cell growth and chemosensitivity.<sup>38,41</sup> Our investigation demonstrated that miR-195 targets *TUBB* to regulate the chemosensitivity of NSCLC cells. Interestingly, although *TUBB* is the most abundant among tubulin proteins, miR-195 regulation of *TUBB* does not alter microtubule structure. In parallel, we found that miR-195 represses lung metastasis *in vivo*, likely by targeting *BIRC5* to regulate the migration and invasion of NSCLC cells. These findings enhance our understanding of the downstream targets of miR-195 and support the application of miR-195 replacement as a therapeutic approach to address both chemoresistance and metastasis.

The correlation between *TUBB* mutations and paclitaxel resistance in NSCLC was debated almost two decades ago.<sup>20–23</sup> Similarly, the

correlation between *TUBB* expression and paclitaxel resistance has also been discussed.<sup>17</sup> However, neither *TUBB* mutations nor expression were found to correlate with NSCLC resistance to paclitaxel, and the role of *TUBB* in chemoresistance has never been experimentally validated. Here, we demonstrate that *TUBB* expression is increased in tumor tissues compared to adjacent normal tissues in lung adenocarcinoma and squamous cell carcinoma patients and that higher expression of *TUBB* is correlated with worse overall survival and poor response to chemotherapy in lung adenocarcinoma patients. Importantly, overexpression of *TUBB* confers resistance to MTAs, while knockdown of *TUBB* sensitizes NSCLC cells to MTAs. These findings demonstrate the oncogenic potential of *TUBB* and support the therapeutic value of targeting *TUBB* to chemosensitize NSCLC. Additionally, we show that *TUBB* is a direct target of miR-195 and can be regulated by another target of miR-195, *CHEK1*. Consistent with this, we found that the expression of *TUBB* is positively associated with the expression of *CHEK1* in lung adenocarcinoma and squamous cell carcinoma tissues.

*BIRC5*, a well characterized oncogene, has been shown to regulate the growth, migration, and invasion of various cancer cells.<sup>25,50,52,53</sup> Strategies to repress survivin have been proposed as attractive treatment options.<sup>54,55</sup> We have recently shown that miR-195 directly targets *BIRC5* to regulate the apoptosis and senescence of NSCLC cells.<sup>33</sup> Here, we report that miR-195 directly targets *BIRC5* to regulate the migration and invasion of NSCLC cells. Our results indicate that the miR-195/survivin axis is one of the major regulators of NSCLC migration and invasion and therefore a candidate target for treatment of NSCLC.

In conclusion, this report demonstrates that miR-195 targets *TUBB* to regulate the response of NSCLC cells to MTAs and that the expression of *TUBB* can be a prognostic factor in lung adenocarcinoma. It reveals



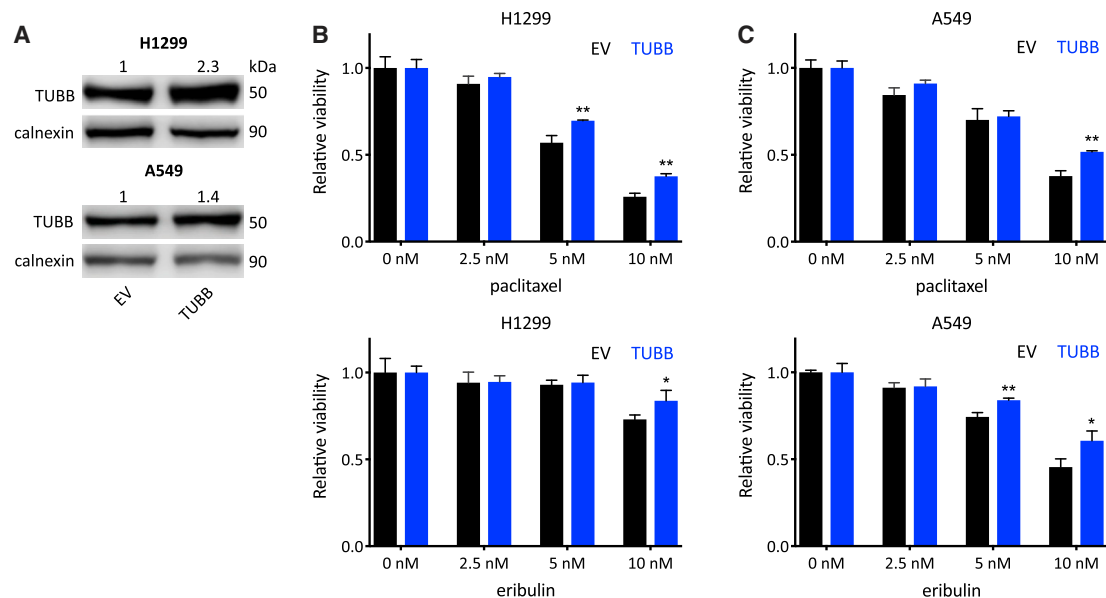


**Figure 4. TUBB Confers Resistance to MTAs in NSCLC Cells**

(A) Protein levels of TUBB assessed by western blot. (B) Response of cells transfected with TUBB-expressing vector to paclitaxel. (C) Response of cells transfected with TUBB-expressing vector to eribulin. Results are shown as mean  $\pm$  SD. \* $p < 0.05$ ; \*\* $p < 0.01$ . Experiments were repeated at least twice.

that *BIRC5* mediates the function of miR-195 to regulate the migration and invasion of NSCLC cells. It also establishes the relevance of the miR-195/TUBB and miR-195/*BIRC5* axis as a focal therapeutic target to simultaneously overcome drug resistance and repress lung cancer metastasis.

## MATERIALS AND METHODS

### Reagents and Cell Lines

Paclitaxel was obtained from Teva Pharmaceutical Industries (PA, USA). Eribulin mesylate (Eisai) was kindly provided by Dr. Peter Houghton. miR-195 mimics were purchased from Dharmacon (CO, USA) and IDT (IA, USA). Two miR-195 inhibitors, IH-300643-05-0005 (miR-195 inh #1) and HSTUD0320 (miR-195 inh #2), were obtained from Dharmacon and Sigma-Aldrich (MO, USA). Two negative control oligomers (oligos) (D-001810-10-05 and CN-001000-01-20) were purchased from Dharmacon. Lipofectamine RNAiMAX and 2000 transfection reagents were purchased from Thermo Fisher Scientific (MA, USA). Oligos were transfected into cells at 25 nM unless otherwise specified.

ON-TARGETplus TUBB SMARTpool siRNAs were purchased from GE Dharmacon (L-010325-00-0005). The targeted sequences include: 5'-GGAAUGGGCACUCUCCUUA-3', 5'-AAGAAUACCUGAUCGCAU-3', 5'-UCCAUCAGUUGGUAGAGAA-3', and 5'-CCGCAUCUCUGUGUACUAC-3'.

Two siRNAs designed against different regions of CHEK1 were purchased from Sigma-Aldrich: SASI\_Hs02\_00326304 was designed to target 5'-CTGAAAGAGACTTGTGAGAA-3' and

SASI\_Hs02\_00326305 was designed to target 5'-TAGATATG AAGCGTGCCGT-3'.

Four NSCLC cell lines—H1299 (large cell carcinoma), H1993, A549, and H358 (lung adenocarcinoma)—were established at the National Cancer Institute and obtained from Dr. John Minna and Adi Gazdar at the Hamon Center for Therapeutic Oncology Research at University of Texas (UT) Southwestern Medical Center in Dallas, TX. All cell lines were grown in RPMI-1640 medium supplemented with 5% fetal bovine serum (FBS) and 1% penicillin/streptomycin. All cell lines were grown in a humidified atmosphere with 5% CO<sub>2</sub> at 37°C, authenticated using short tandem repeat profiling, and confirmed to be mycoplasma-free through PCR. Cells were discarded when they were close to passage 20.

H1299/control, H1299/miR-195, 344SQ/control, and 344SQ/miR-195 cells were generated using luciferase-pcDNA3, which was a gift from William Kaelin (Addgene plasmid #18964). TUBB cDNA was cloned from pLX304-TUBB (DNASU, HsCD00435210) and inserted into pIRESpuro3 (Catalog #631669, Clontech, CA, USA).

### Cell Viability Assays

Cells were plated in 96-well format and/or transfected with oligos in different concentrations. After incubating for 24–48 h, cells were further treated with medium or different concentrations of drugs. After a total incubation of 120 h, cell viability was determined using the CellTiter-Glo cell viability assay (Promega). Dose-response curves were generated using GraphPad Prism 7 (CA, USA).

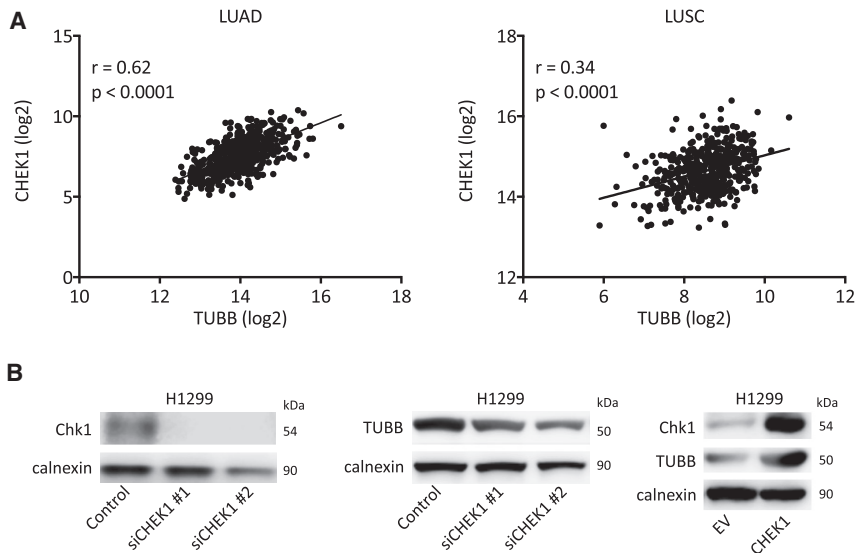


**Figure 5. TUBB Is Regulated by CHEK1**

(A) Correlation of *TUBB* with *CHEK1* in tumor tissues of lung adenocarcinoma ( $n = 507$ ) and lung squamous cell carcinoma ( $n = 475$ ) patients. (B) *CHEK1* and *TUBB* protein levels assessed by western blots. Experiments were repeated at least twice.

### RNA Extraction and qRT-PCR

Total RNA was prepared using the mirVana miRNA Isolation Kit (Ambion) according to manufacturer's instructions. Intracellular miRNA levels were assessed by qRT-PCR on an ABI ViiA7 System using miRNA expression assay primer and probe sets (Applied Biosystems). RNU44, RNU66, or U6 were used as controls for normalization of miRNA expression. mRNA levels were assessed by qRT-PCR on an ABI ViiA7 System using SYBR Green (Thermo Fisher) and primers designed by IDT and purchased from Sigma. *GAPDH* expression was used as a control for normalization of mRNA expression. Threshold

cycle times (Ct) were obtained, and relative gene expression was calculated using the comparative cycle time method. Primers used for *GAPDH*: forward-5'-GAAGGTGAAGGTCGGAGTC-3' and reverse-5'-GAAGATGGTGTGGGATTTC-3'. Primers used for *TUBB*: forward-5'-TGGTAG AAGGTAGTGGGTAGAA-3' and reverse-5'-GAGGTAGAGTTGGAAGGGAAG-3'.

### Luciferase Reporter Assay

Luciferase reporter assays were performed as previously reported.<sup>56</sup> Mutant constructs were generated with the seed target sites mutated or deleted as specified in Results. H1299 cells were maintained in 96-well plates and co-transfected with luciferase reporters (0.05  $\mu\text{g}/\text{well}$ ) and miRNA mimics or control oligo (15 nM). Luciferase activities were measured 72 h later using the Dual-Glo Luciferase Assay System (Promega). Firefly luciferase was normalized to sea pansy luciferase activity to evaluate the regulatory effect of miR-195 on its putative targets. Primers used for *TUBB* 3' UTR: forward-5'-GTTATCAGA GCTCGACCAGCCTTGGTCCCTAAGCC-3' and reverse-5'-CAT TTGCTCGAGCAGCTTTTTTCAATTCCCATTATTATTTTGG-3'.

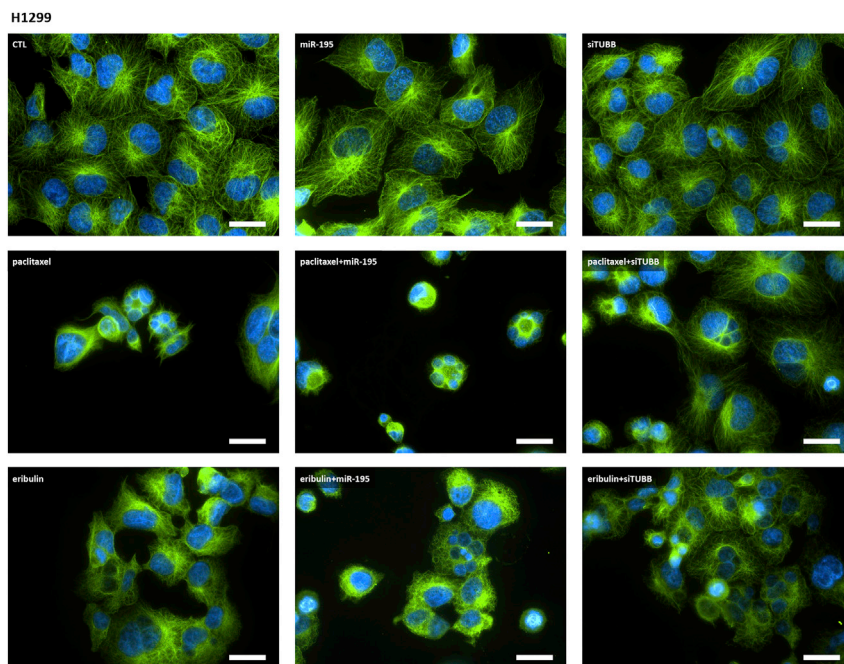


**Figure 6. miR-195 Has No Effect on Microtubule Structure**

Cells were treated with different conditions (20 nM oligos and/or 10 nM paclitaxel/eribulin) and stained with antibodies against tubulin (green) and DAPI (blue). Pictures were taken under 60 $\times$  magnification, and scale bars represent 20  $\mu\text{m}$ . Experiments were repeated at least twice.

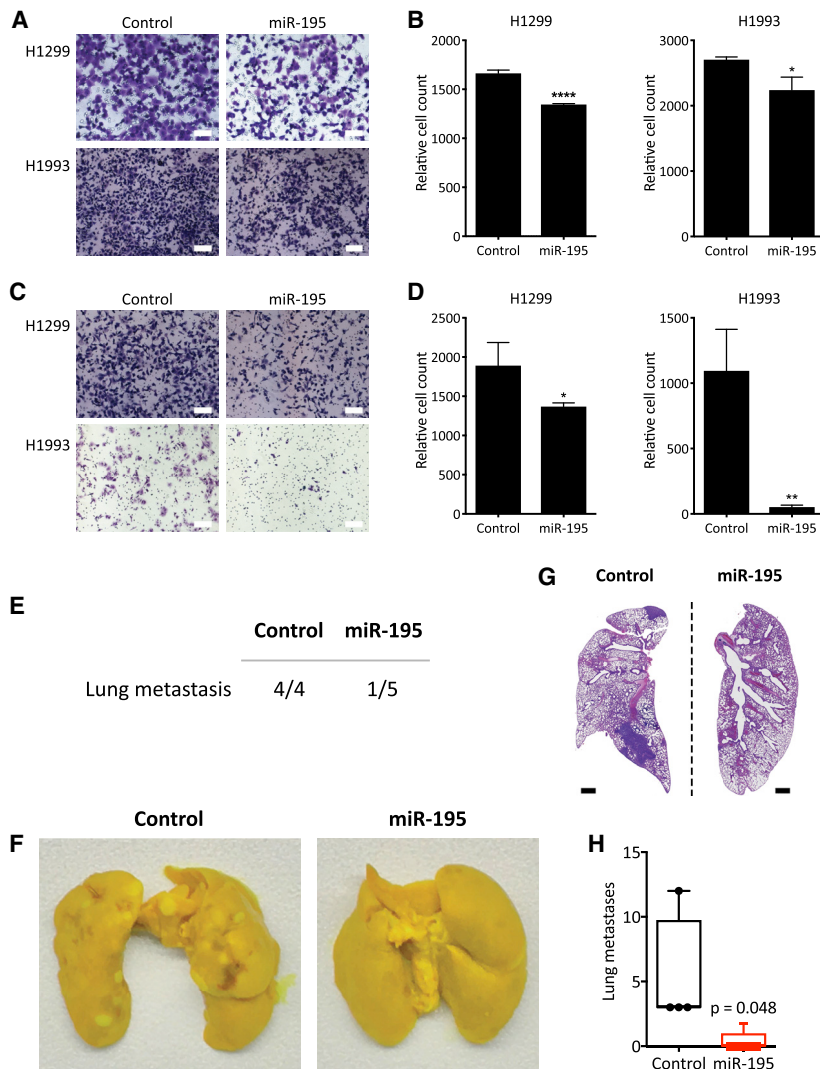


**Figure 7. miR-195 Represses Metastasis of NSCLC**

(A) Migration assay in H1299 and H1993 cells transfected with control oligo (NC) or miR-195. (B) Quantification of migration assay. (C) Matrigel invasion assay in H1299 and H1993 cells transfected with negative control oligo or miR-195. (D) Quantification of invasion assay. (E) Number of mice shown signs of lung metastasis in control and miR-195 group. (F) Representative images of the lungs in control and miR-195 group fixed with Bouin's solution. (G) Representative H&E images of the left lung in control group and right lung in miR-195 group. (H) Quantification of lung metastasis nodules. Results are shown as mean  $\pm$  SD. \* $p < 0.05$ ; \*\* $p < 0.01$ ; \*\*\*\* $p < 0.0001$ . Cell migration and invasion images were acquired with a 10 $\times$  objective and scale bars correspond to 100  $\mu$ m. Lung H&E staining images were acquired at 4 $\times$ , and scale bars represent 1 mm. Except for mouse experiments, all other experiments were repeated at least twice.

peroxidase (HRP) (Santa Cruz Biotechnology) and visualized by enhanced chemiluminescent (ECL) substrate (Pierce/Thermo Fisher Scientific) on an Odyssey Fc Imaging System (LI-COR). All western blots were repeated at least twice.

#### Migration and Invasion Assay

Cell migration was assessed using the Boyden chamber assay. After being transfected with oligos as specified, cells in serum-free medium were seeded into the upper chamber of 8- $\mu$ m pore size inserts (Corning). The inserts were placed into the wells of a 24-well plate with media containing 10% FBS. The invasion assay was similarly set up, except that the inserts were coated with Matrigel. After 24 h incubation, cells that migrated through the membrane or invaded

through the Matrigel into the lower chamber of the inserts were fixed with ethanol and stained with crystal violet. Pictures were taken from five randomly selected visual fields, and cells were counted using ImageJ (NIH). Chemotaxis was assayed in a similar manner. After seeding cells into a ClearView plate (Essen), cells migrating or invading to the lower chamber of the inserts were recorded using an IncuCyte Zoom live cell imaging system (Essen BioScience).

#### Animal Experiments

Animal protocols were approved by the Institutional Animal Care and Use Committee of the UT Health Science Center at San Antonio. Six- to seven-week-old female athymic nude Foxn1nu (nu/nu) mice were purchased from Envigo. Five- to seven-week-old female 129/SV mice were purchased from Charles River.  $1 \times 10^6$  cells in 200  $\mu$ L PBS/Matrigel (v/v, 1:1) were injected subcutaneously into the flanks of the mice. Mice were randomized into different groups without blinding. Tumor volumes were measured using calipers

Primers used for *TUBB* 3' UTR with mutations in the binding site of miR-195: forward-5'-GTTGAACTTGAGAGTTTTTTTCATAT TGAAAAGATGACATCGCC-3' and reverse-5'-AAAAACTCTCAA GTTCAACATAAAATAGAAATCTCAAATGTAGGATAGAA-3'.

#### Western Blots

Cell lysates were prepared using radioimmunoprecipitation assay (RIPA) buffer. Equal amounts of lysate were resolved by SDS-PAGE and transferred to ImmunBlot polyvinylidene difluoride (PVDF) membranes (Bio-Rad). Membranes were blocked and probed with specific primary antibodies. Anti-Chk1 (A300-161A-T) was purchased from Bethyl Laboratories (TX, USA). Antibodies to calnexin (sc-11397) and GAPDH (sc-25778) were purchased from Santa Cruz Biotechnology (TX, USA). Anti-actin (4970P) was purchased from Cell Signaling Technology (MA, USA). Anti-TUBB (T7816-100UL) was purchased from Sigma (MO, USA). Bound antibodies were detected with secondary antibodies conjugated with horseradish



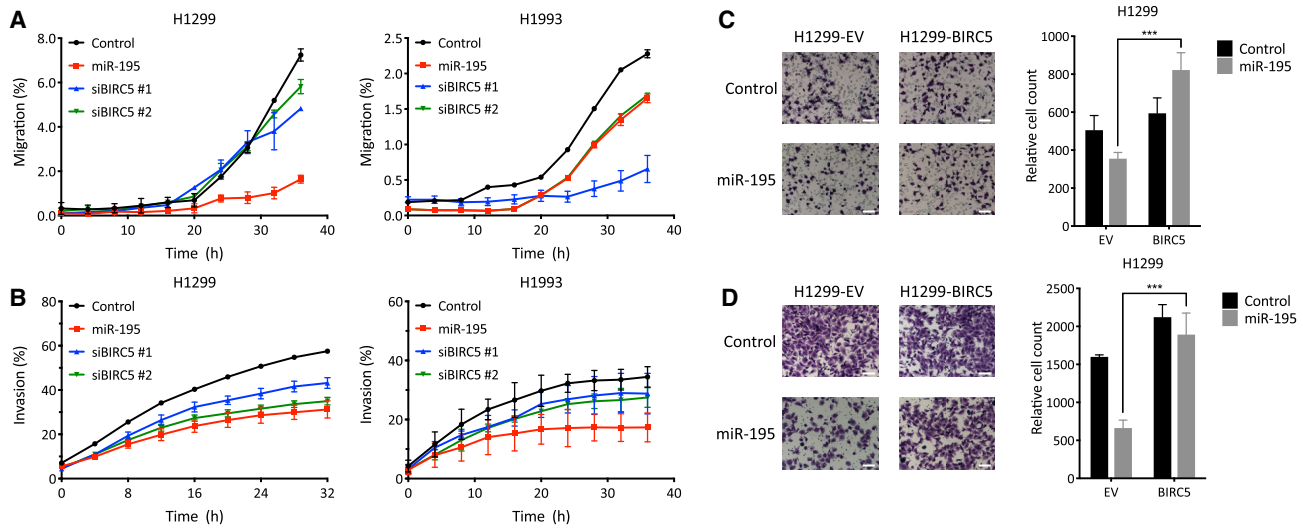


**Figure 8. BIRC5 Reverses the Repression of Migration and Invasion by miR-195**

(A) Effect of miR-195 and siBIRC5 on the migration of H1299 and H1993 cells assessed by chemotaxis assay. (B) Effect of miR-195 and siBIRC5 on the invasion of H1299 and H1993 cells assessed by chemotaxis invasion assay. (C) Overexpression of BIRC5 rescues the migration of cancer cells transfected with miR-195. (D) Overexpression of BIRC5 rescues the invasion of cancer cells transfected with miR-195. Results are shown as mean  $\pm$  SD. \*\*\* $p < 0.001$ . Cell migration and invasion images were acquired with a 10 $\times$  objective and scale bars correspond to 100  $\mu$ m. Experiments were repeated at least twice.

and calculated by the formula volume =  $1/2 \times \text{width}^2 \times \text{length}$ . For tail vein injections,  $1 \times 10^6$  cells were injected via the lateral tail vein. Growth of lung metastases was monitored via IVIS Spectrum *In Vivo* Imaging System (CA, USA).

#### Statistical Analysis

Mean values between groups were compared by Student's two-sided *t* test as implemented in GraphPad Prism 7, with  $p < 0.05$  considered statistically significant. Results are representative of 2 to 4 individual experiments or as indicated in the figures. Differences in mouse body weight over time were compared by two-way ANOVA.

#### SUPPLEMENTAL INFORMATION

Supplemental Information can be found online at <https://doi.org/10.1016/j.omto.2019.07.004>.

#### AUTHOR CONTRIBUTIONS

X.Y. and A.P. were involved in study concept and design; acquisition, analysis, and interpretation of data; and drafting of the manuscript. Y.Z. and B.W. were involved in acquisition and analysis of data. J.M.K. provided materials and was involved in critical revision of the manuscript for important intellectual content. A.P. supervised the study, obtained funding, provided material support, and was involved in study concept and design, drafting of the manuscript, critical revision of the manuscript for important intellectual content, and statistical analysis. All authors read and approved the final manuscript.

#### CONFLICTS OF INTEREST

The authors declare no competing interests.

#### ACKNOWLEDGMENTS

This work was supported the NIH (R01 CA129632 and P30 CA054174) and the Cancer Prevention and Research Institute of Texas (Research Training Award RP140105).

#### REFERENCES

1. Siegel, R.L., Miller, K.D., and Jemal, A. (2016). Cancer statistics, 2016. *CA Cancer J. Clin.* 66, 7–30.
2. Fossella, F.V. (2002). Docetaxel for previously treated non-small-cell lung cancer. *Oncology (Williston Park)* 16 (6, Suppl 6), 45–51.
3. Rosell, R., Gatzemeier, U., Betticher, D.C., Keppler, U., Macha, H.N., Pirker, R., Berthet, P., Breau, J.L., Lianes, P., Nicholson, M., et al. (2002). Phase III randomised trial comparing paclitaxel/carboplatin with paclitaxel/cisplatin in patients with advanced non-small-cell lung cancer: a cooperative multinational trial. *Ann. Oncol.* 13, 1539–1549.
4. Rowinsky, E.K., and Donehower, R.C. (1995). Paclitaxel (taxol). *N. Engl. J. Med.* 332, 1004–1014.
5. Chang, A. (2011). Chemotherapy, chemoresistance and the changing treatment landscape for NSCLC. *Lung Cancer* 71, 3–10.
6. Gupta, G.P., and Massagué, J. (2006). Cancer metastasis: building a framework. *Cell* 127, 679–695.
7. Kartner, N., Riordan, J.R., and Ling, V. (1983). Cell surface P-glycoprotein associated with multidrug resistance in mammalian cell lines. *Science* 221, 1285–1288.
8. Horwitz, S.B., Cohen, D., Rao, S., Ringel, I., Shen, H.J., and Yang, C.P. (1993). Taxol: mechanisms of action and resistance. *J. Natl. Cancer Inst. Monogr.* 15, 55–61.
9. Shen, D.W., Fojo, A., Chin, J.E., Roninson, I.B., Richert, N., Pastan, I., and Gottesman, M.M. (1986). Human multidrug-resistant cell lines: increased *mdr1* expression can precede gene amplification. *Science* 232, 643–645.
10. Fojo, T., and Menefee, M. (2007). Mechanisms of multidrug resistance: the potential role of microtubule-stabilizing agents. *Ann. Oncol.* 18 (Suppl 5), v3–v8.
11. Komlodi-Pasztor, E., Sackett, D., Wilkerson, J., and Fojo, T. (2011). Mitosis is not a key target of microtubule agents in patient tumors. *Nat. Rev. Clin. Oncol.* 8, 244–250.

12. Gonçalves, A., Braguer, D., Kamath, K., Martello, L., Briand, C., Horwitz, S., Wilson, L., and Jordan, M.A. (2001). Resistance to Taxol in lung cancer cells associated with increased microtubule dynamics. *Proc. Natl. Acad. Sci. USA* 98, 11737–11742.
13. Xiao, Z., Xue, J., Semizarov, D., Sowin, T.J., Rosenberg, S.H., and Zhang, H. (2005). Novel indication for cancer therapy: Chk1 inhibition sensitizes tumor cells to antimetotics. *Int. J. Cancer* 115, 528–538.
14. Lee, J.H., Choy, M.L., Ngo, L., Venta-Perez, G., and Marks, P.A. (2011). Role of checkpoint kinase 1 (Chk1) in the mechanisms of resistance to histone deacetylase inhibitors. *Proc. Natl. Acad. Sci. USA* 108, 19629–19634.
15. Gan, P.P., Pasquier, E., and Kavallaris, M. (2007). Class III beta-tubulin mediates sensitivity to chemotherapeutic drugs in non small cell lung cancer. *Cancer Res.* 67, 9356–9363.
16. Vilmar, A.C., Santoni-Rugiu, E., and Sørensen, J.B. (2011). Class III  $\beta$ -tubulin in advanced NSCLC of adenocarcinoma subtype predicts superior outcome in a randomized trial. *Clin. Cancer Res.* 17, 5205–5214.
17. Lee, K.M., Cao, D., Itami, A., Pour, P.M., Hruban, R.H., Maitra, A., and Ouellette, M.M. (2007). Class III beta-tubulin, a marker of resistance to paclitaxel, is overexpressed in pancreatic ductal adenocarcinoma and intraepithelial neoplasia. *Histopathology* 51, 539–546.
18. Stengel, C., Newman, S.P., Leese, M.P., Potter, B.V., Reed, M.J., and Purohit, A. (2010). Class III beta-tubulin expression and in vitro resistance to microtubule targeting agents. *Br. J. Cancer* 102, 316–324.
19. Narvi, E., Jaakkola, K., Winsel, S., Oetken-Lindholm, C., Halonen, P., Kallio, L., and Kallio, M.J. (2013). Altered TUBB3 expression contributes to the epothilone response of mitotic cells. *Br. J. Cancer* 108, 82–90.
20. Monzó, M., Rosell, R., Sánchez, J.J., Lee, J.S., O'Brate, A., González-Larriba, J.L., Alberola, V., Lorenzo, J.C., Núñez, L., Ro, J.Y., and Martín, C. (1999). Paclitaxel resistance in non-small-cell lung cancer associated with beta-tubulin gene mutations. *J. Clin. Oncol.* 17, 1786–1793.
21. Kelley, M.J., Li, S., and Harpole, D.H. (2001). Genetic analysis of the beta-tubulin gene, TUBB, in non-small-cell lung cancer. *J. Natl. Cancer Inst.* 93, 1886–1888.
22. Monzo, M., Taron, M., and Rosell, R. (2002). Re: Genetic analysis of the beta-tubulin gene, TUBB, in non-small-cell lung cancer. *J. Natl. Cancer Inst.* 94, 774–776, author reply 777.
23. Sale, S., Oefner, P.J., and Sikic, B.I. (2002). Re: genetic analysis of the beta-tubulin gene, TUBB, in non-small-cell lung cancer. *J. Natl. Cancer Inst.* 94, 776–777, author reply 777.
24. Zhang, W., Liu, Y., Li, Y.F., Yue, Y., Yang, X., and Peng, L. (2016). Targeting of Survivin Pathways by YM155 Inhibits Cell Death and Invasion in Oral Squamous Cell Carcinoma Cells. *Cell. Physiol. Biochem.* 38, 2426–2437.
25. Kogo, R., How, C., Chaudary, N., Bruce, J., Shi, W., Hill, R.P., Zahedi, P., Yip, K.W., and Liu, F.F. (2015). The microRNA-218~Survivin axis regulates migration, invasion, and lymph node metastasis in cervical cancer. *Oncotarget* 6, 1090–1100.
26. Chen, X., Zhang, Y., Tang, C., Tian, C., Sun, Q., Su, Z., Xue, L., Yin, Y., Ju, C., and Zhang, C. (2017). Co-delivery of paclitaxel and anti-survivin siRNA via redox-sensitive oligopeptide liposomes for the synergistic treatment of breast cancer and metastasis. *Int. J. Pharm.* 529, 102–115.
27. Chu, X.Y., Chen, L.B., Wang, J.H., Su, Q.S., Yang, J.R., Lin, Y., Xue, L.J., Liu, X.B., and Mo, X.B. (2012). Overexpression of survivin is correlated with increased invasion and metastasis of colorectal cancer. *J. Surg. Oncol.* 105, 520–528.
28. Ye, Q., Cai, W., Zheng, Y., Evers, B.M., and She, Q.B. (2014). ERK and AKT signaling cooperate to translationally regulate survivin expression for metastatic progression of colorectal cancer. *Oncogene* 33, 1828–1839.
29. McKenzie, J.A., Liu, T., Jung, J.Y., Jones, B.B., Ekiz, H.A., Welm, A.L., and Grossman, D. (2013). Survivin promotion of melanoma metastasis requires upregulation of  $\alpha 5$  integrin. *Carcinogenesis* 34, 2137–2144.
30. Ambrosini, G., Adida, C., and Altieri, D.C. (1997). A novel anti-apoptosis gene, survivin, expressed in cancer and lymphoma. *Nat. Med.* 3, 917–921.
31. Monzó, M., Rosell, R., Felip, E., Astudillo, J., Sánchez, J.J., Maestre, J., Martín, C., Font, A., Barnadas, A., and Abad, A. (1999). A novel anti-apoptosis gene: Re-expression of survivin messenger RNA as a prognosis marker in non-small-cell lung cancers. *J. Clin. Oncol.* 17, 2100–2104.
32. Olie, R.A., Simões-Wüst, A.P., Baumann, B., Leech, S.H., Fabbro, D., Stahel, R.A., and Zangemeister-Wittke, U. (2000). A novel antisense oligonucleotide targeting survivin expression induces apoptosis and sensitizes lung cancer cells to chemotherapy. *Cancer Res.* 60, 2805–2809.
33. Yu, X., Zhang, Y., Cavazos, D., Ma, X., Zhao, Z., Du, L., and Pertsemidlis, A. (2018). miR-195 targets cyclin D3 and survivin to modulate the tumorigenesis of non-small cell lung cancer. *Cell Death Dis.* 9, 193.
34. Chen, K., and Rajewsky, N. (2007). The evolution of gene regulation by transcription factors and microRNAs. *Nat. Rev. Genet.* 8, 93–103.
35. Qu, J., Zhao, L., Zhang, P., Wang, J., Xu, N., Mi, W., Jiang, X., Zhang, C., and Qu, J. (2015). MicroRNA-195 chemosensitizes colon cancer cells to the chemotherapeutic drug doxorubicin by targeting the first binding site of BCL2L2 mRNA. *J. Cell. Physiol.* 230, 535–545.
36. Shen, C.J., Cheng, Y.M., and Wang, C.L. (2017). LncRNA PVT1 epigenetically silences miR-195 and modulates EMT and chemoresistance in cervical cancer cells. *J. Drug Target.* 25, 637–644.
37. Ujifuku, K., Mitsutake, N., Takakura, S., Matsuse, M., Saenko, V., Suzuki, K., Hayashi, K., Matsuo, T., Kamada, K., Nagata, I., and Yamashita, S. (2010). miR-195, miR-455-3p and miR-10a( \*) are implicated in acquired temozolomide resistance in glioblastoma multiforme cells. *Cancer Lett.* 296, 241–248.
38. Yu, X., Zhang, Y., Ma, X., and Pertsemidlis, A. (2018). miR-195 potentiates the efficacy of microtubule-targeting agents in non-small cell lung cancer. *Cancer Lett.* 427, 85–93.
39. Fu, M.G., Li, S., Yu, T.T., Qian, L.J., Cao, R.S., Zhu, H., Xiao, B., Jiao, C.H., Tang, N.N., Ma, J.J., et al. (2013). Differential expression of miR-195 in esophageal squamous cell carcinoma and miR-195 expression inhibits tumor cell proliferation and invasion by targeting of Cdc42. *FEBS Lett.* 587, 3471–3479.
40. Li, D., Zhao, Y., Liu, C., Chen, X., Qi, Y., Jiang, Y., Zou, C., Zhang, X., Liu, S., Wang, X., et al. (2011). Analysis of MiR-195 and MiR-497 expression, regulation and role in breast cancer. *Clin. Cancer Res.* 17, 1722–1730.
41. Liu, B., Qu, J., Xu, F., Guo, Y., Wang, Y., Yu, H., and Qian, B. (2015). MiR-195 suppresses non-small cell lung cancer by targeting CHEK1. *Oncotarget* 6, 9445–9456.
42. Mao, J.H., Zhou, R.P., Peng, A.F., Liu, Z.L., Huang, S.H., Long, X.H., and Shu, Y. (2012). microRNA-195 suppresses osteosarcoma cell invasion and migration in vitro by targeting FASN. *Oncol. Lett.* 4, 1125–1129.
43. Wang, R., Zhao, N., Li, S., Fang, J.H., Chen, M.X., Yang, J., Jia, W.H., Yuan, Y., and Zhuang, S.M. (2013). MicroRNA-195 suppresses angiogenesis and metastasis of hepatocellular carcinoma by inhibiting the expression of VEGF, VAV2, and CDC42. *Hepatology* 58, 642–653.
44. Bhattacharya, A., Schmitz, U., Wolkenhauer, O., Schönherr, M., Raatz, Y., and Kunz, M. (2013). Regulation of cell cycle checkpoint kinase WEE1 by miR-195 in malignant melanoma. *Oncogene* 32, 3175–3183.
45. Györfy, B., Surowiak, P., Budczies, J., and Lánckzy, A. (2013). Online survival analysis software to assess the prognostic value of biomarkers using transcriptomic data in non-small-cell lung cancer. *PLoS ONE* 8, e82241.
46. Yongchun, Z., Linwei, T., Xicai, W., Lianhua, Y., Guangqiang, Z., Ming, Y., Guanjian, L., Yujie, L., and Yunchao, H. (2014). MicroRNA-195 inhibits non-small cell lung cancer cell proliferation, migration and invasion by targeting MYB. *Cancer Lett.* 347, 65–74.
47. Zhang, S., Yuan, J., and Zheng, R. (2016). Suppression of Ubiquitin-Specific Peptidase 17 (USP17) Inhibits Tumorigenesis and Invasion in Non-Small Cell Lung Cancer Cells. *Oncol. Res.* 24, 263–269.
48. Singla, A.K., Downey, C.M., Bebb, G.D., and Jirik, F.R. (2015). Characterization of a murine model of metastatic human non-small cell lung cancer and effect of CXCR4 inhibition on the growth of metastases. *Oncoscience* 2, 263–271.
49. Gibbons, D.L., Lin, W., Creighton, C.J., Rizvi, Z.H., Gregory, P.A., Goodall, G.J., Thilaganathan, N., Du, L., Zhang, Y., Pertsemidlis, A., and Kurie, J.M. (2009). Contextual extracellular cues promote tumor cell EMT and metastasis by regulating miR-200 family expression. *Genes Dev.* 23, 2140–2151.
50. Altieri, D.C. (2008). Survivin, cancer networks and pathway-directed drug discovery. *Nat. Rev. Cancer* 8, 61–70.

51. Unruhe, B., Schröder, E., Wünsch, D., and Knauer, S.K. (2016). An Old Flame Never Dies: Survivin in Cancer and Cellular Senescence. *Gerontology* 62, 173–181.
52. Altieri, D.C. (2003). Survivin, versatile modulation of cell division and apoptosis in cancer. *Oncogene* 22, 8581–8589.
53. Wang, Q., Wu, P.C., Roberson, R.S., Luk, B.V., Ivanova, I., Chu, E., and Wu, D.Y. (2011). Survivin and escaping in therapy-induced cellular senescence. *Int. J. Cancer* 128, 1546–1558.
54. Pennati, M., Folini, M., and Zaffaroni, N. (2007). Targeting survivin in cancer therapy: fulfilled promises and open questions. *Carcinogenesis* 28, 1133–1139.
55. Altieri, D.C. (2001). The molecular basis and potential role of survivin in cancer diagnosis and therapy. *Trends Mol. Med.* 7, 542–547.
56. Zhao, Z., Ma, X., Hsiao, T.H., Lin, G., Kosti, A., Yu, X., Suresh, U., Chen, Y., Tomlinson, G.E., Pertsemlidis, A., and Du, L. (2014). A high-content morphological screen identifies novel microRNAs that regulate neuroblastoma cell differentiation. *Oncotarget* 5, 2499–2512.